Author Manuscript

Author Manuscript

Author Manuscript

Author Manuscript

HHS Public Access

Author manuscript

Itch (Phila). Author manuscript; available in PMC 2021 January 12.

Published in final edited form as:

Itch (Phila). 2019 ; 4(3): . doi:10.1097/itx.0000000000000028.

MrgprX1 Mediates Neuronal Excitability and Itch Through Tetrodotoxin-Resistant Sodium Channels

Pang-Yen Tseng[1], **Qin Zheng**[1], **Zhe Li**[1], **Xinzhong Dong**[1,2]

[1]The Solomon H. Snyder Department of Neuroscience and Center for Sensory Biology, Johns Hopkins University School of Medicine, Baltimore, MD 21205, USA

[2]Howard Hughes Medical Institute, Johns Hopkins University School of Medicine, Baltimore, MD 21205, USA.

Abstract

In this study, we sought to elucidate the molecular mechanism underlying human Mas-related G protein-coupled receptor X1 (MrgprX1) mediated itch sensation. We found that activation of MrgprX1 by BAM8-22 triggered robust action potential discharges in dorsal root ganglion (DRG) neurons. This neuronal excitability is not mediated by Transient receptor potential (TRP) cation channels, M-type potassium channels, or chloride channels. Instead, activation of MrgprX1 lowers the activation threshold of TTX-resistant sodium channels and induces inward sodium currents. These MrgprX1-elicited action potential discharges can be blocked by Pertussis toxin (PTX) and a Gβγ inhibitor – Gallein. Behavioral results showed that Nav1.9 knockout but not Trpa1 knockout significantly reduced BAM8-22 evoked scratching behavior. Collectively, these data suggest that activation of MrgprX1 triggers itch sensation by increasing the activity of TTX-resistant voltage-gated sodium channels.

Keywords

MrgprX1; BAM8-22; itch; dorsal root ganglion neurons; TTX-resistant sodium channels; TRPA1; TRPV1

Introduction

Mas-related G-protein coupled receptors represent a large family of receptors that play important roles in various somatosensory functions including itch, pain, and allergy[1-3]. MrgprX1, a primate-specific Mrgprs, is a pruritogenic receptor expressed in the peripheral sensory system. In humans, application of a MrgprX1 agonist – Bovine adrenal medulla peptide 8–22 (BAM8–22), a proteolytically cleaved product of proenkephalin A, onto skin

Correspondence: Xinzhong Dong, PhD, The Johns Hopkins University, Phone: 410-502-2993; Fax: 410-614-6249; xdong2@jhmi.edu.

Author Contributions

Pang-Yen Tseng: designing and performing electrophysiological experiments, analyzing data, and writing draft. Qin Zheng: designing and performing behavioral experiment of Trpa1 knockout mice. Zhe Li: designing and performing behavioral test of Nav1.9 knockout mice. Xinzhong Dong: supervision, resources, funding acquisition, reviewing and editing draft.

Competing interests

Xinzhong Dong has a financial interest in Escient Pharmaceuticals a company focused on developing small molecule inhibitors for MRGPRs. The other authors declare that no competing interests exist.

Author Manuscript Author Manuscript Author Manuscript Author Manuscript

induces acute itch accompanied by other nociceptive responses including pricking, stinging and burning [4]. Human MrgprX1 shares some features of mouse MrgprC11 and it is thought that MrgprC11 and MrgprA3 evoke itch sensation by opening transient receptor potential ankyrin 1 (Trpa1) in a phospholipase C (PLC) dependent pathway [5]. However, whether MrgprX1 shares this same mechanism is still unknown. Although murine MrgprC11 is considered analogous to human MrgprX1 due to their common agonist BAM8–22, MrgprC11 and MrgprX1 in fact show distinct pharmacological properties and trigger different signaling cascades. For example, Chloroquine activates MrgprX1 but not MrgprC11 [6], γ_2-melanocyte stimulating hormone (γ_2-MSH), dynorphin-14, neuropeptide FF or neuropeptide AF activate MrgprC11 but not MrgprX1[1,7]; a small molecule 2-(cyclopropanesulfonamido)-N-(2-ethoxyphenyl) benzamide allosterically modulates MrgprX1 but not MrgprC11 [8(p38),9]. Mechanistically studying MrgprX1 is challenging because there is no mouse homolog. In this study, we used a recently developed "humanized" mouse model in which twelve endogenous murine Mrgprs (including MrgprA3 and MrgprC11) were replaced by human MrgprX1, to study its function in native dorsal root ganglion neurons. We found that MrgprX1-mediated neuronal excitability and itch behavior does not require the Trpa1 channel. Instead, it is likely through direct modulation of TTX-resistant sodium channels.

Materials and methods

Animal care and use

All experiments were performed in accordance with protocols approved by the Animal Care and Use Committee at the Johns Hopkins University School of Medicine.

Generation of MrgprX1 transgenic mouse line

All animal experiments were performed under protocols approved by the Animal Care and Use Committee of the Johns Hopkins University School of Medicine. The generation of humanized MrgprX1 mouse line is described in previous report [9]. Briefly, we generated a bacterial artificial chromosome transgenic MrgprX1 mouse line. The expression of MrgprX1 is driven by murine MrgprC11 because of the homology between these two genes. To label the MrgprX1 neurons, the MrgprC11 $^{\text{MrgprX1}}$ mouse line was mated with MrgprA3 $^{\text{GFP-cre}}$ mouse line. The MrgprC11 $^{\text{MrgprX1}}$ / MrgprA3 $^{\text{GFP-cre}}$ mice were mated with Mrgpr $^{-/-}$ mice to remove 12 endogenous murine Mrgprs including MrgprC11 and MrgprA3. Since MrgprA3 and MrgprC11 are coexpressed in a subset of DRG neurons [10], the neurons expressing Cre-GFP are MrgprX1$^+$ neurons (Fig. 1A).

DRG neuron dissociation and culture

Acutely dissociated DRG neurons from adult mice (4weeks old) were collected in cold DH10 (90% Dulbecco's Modified Eagle Medium/F-12, 10% fetal bovine serum, 100 U/mL penicillin, and 100μg/mL streptomycin (Invitrogen, Grand Island, NY, USA) and treated with enzyme solution (5mg/mL dispase, 1mg/mL collagenase Type I in Dulbecco's phosphate-buffered saline (DPBS) without Ca2+ and Mg2+, Invitrogen) at 37°C for 30minutes. After trituration and centrifugation, cells were resuspended in DH10, plated on glass coverslips coated with poly-d-lysine and laminin, and cultured in an incubator (95%

Author Manuscript Author Manuscript Author Manuscript Author Manuscript

O2 and 5% CO2) at 37°C for 24hours with nerve growth factor (25ng/mL) and glial cell-derived neurotrophic factor (50ng/mL).

Electrophysiological recording and data analysis

Whole cell current and voltage clamps were performed on DRG neurons expressing Cre-GFP (Figure 1C). Data were recorded with Axon 700B amplifier and pCLAMP 9.2 software (Molecular Devices, Sunnyvale, CA, USA). Electrodes were pulled (Model pp-830; Narishige, East Meadow, NY, USA) from borosilicate glass (WPI, Inc., Sarasota, FL, USA) with resistances of 2–4 MΩ. Each condition was replicated from at least two mice. In every batch of neurons, control recordings (100nM BAM8–22) were performed to ensure neurons were in health status.

For BAM8–22 elicited neuronal firing under both current and voltage clamps, extracellular solution contained (in mM) 140 NaCl, 4 KCl, 2 $CaCl_2$, 1 $MgCl_2$, 10 HEPES, and 10 Glucose with pH of 7.4 and Osmolality 310 mOsm/kg. Pipette solution contained 140 KCl, 1 $MgCl_2$, 1 EGTA, 10 HEPES, 3 ATP, and 0.5 GTP with pH of 7.4 and osmolality of 300 mOsm/kg.

For TTX-resistant sodium current recordings, extracellular solution contained 35 NaCl, 105 N-methyl-D-glucamine chloride (NMDG-Cl), 0.1 CdCl2, 1 MgCl2, 10 HEPES, and 10 Glucose. Pipette solution contained 140 Tetraethylammonium chloride (TEA-Cl), 10 EGTA, 1 $MgCl_2$, 10 HEPES, 0.5 GTP, and 3 ATP. To isolate TTX-resistant sodium currents, neurons were held at −80 mV followed by 500 ms, −50 mV pre-pulse to inactivated TTX-sensitive sodium channel[11]. Whole cell currents were evoked by 50 ms depolarization pulse ranging from −80mV to 0mV with 10 mV increment. For voltage dependent activation, conductance G was calculated with $G = I_{peak} / (V_{test} - V_{rev})$, where I_{peak} is the peak current, V_{test} is the testing voltage and V_{rev} is reversal potential. Conductance – voltage relationship (G-V curve) was determined by plotting normalized G as the function of V_{test}. The G-V curves were fitted with Boltzmann equation:

$$G(V) = Gmin + \frac{Gmax - Gmin}{1 + e\frac{V - Vhalf}{k}}$$

Where V_{half} is the membrane potentials at which 50% of the channels are open or inactivated and *k* is the slope factor. The current-voltage relations (I-V curves) were measured by plotting peak currents to the testing voltages which were then fitted either by Boltzmann IV equation.

$$I(V) = \frac{(V - Vrev) * Gmax}{1 + e\frac{V - Vhalf}{k}}$$

I(V) is ionic current as the function of membrane voltage. V_{rev} is reversal potential, G_{max} is maximum conductance, V_{half} is the voltage at which half maximum current is, and k is a default slope factor.

Author Manuscript Author Manuscript Author Manuscript Author Manuscript

For voltage-gated calcium current recordings, extracellular solution contained (in mM) 130 N-methyl-D-glucamine chloride (NMDG-Cl), 5 $BaCl_2$, 1 $MgCl_2$, 10 HEPES, and 10 glucose, with pH of 7.4 adjusted with 1 M NMDG. Pipette solution contained (in mM) 140 tetraethylammonium chloride, 10 EGTA, 1 $MgCl_2$, 10 HEPES, 0.5 GTP, and 3 ATP, with pH of 7.4. The voltage protocol was modified from a previously published method [12]. Briefly, cells were held at −80 mV and evoked to −40 mV for 20 milliseconds (ms) to activate low-voltage activated calcium channels, and then held to −60 mV for 20 ms and evoked to −10 mV for 40 ms to activate high-voltage activated calcium channels. Leak currents were subtracted with P/4 protocol.

For M-type potassium current recordings, external solution contained 140 NaCl, 4 KCl, 2 $CaCl_2$, 1 $MgCl_2$, 10 HEPES, and 10 Glucose, and pipette solution contained 140 KCl, 1 $MgCl_2$, 10 EGTA, 10 HEPES, 3 ATP, and 0.5 GTP with pH of 7.4. Neurons were held at −30mV to inactivate other potassium channels and then stepped to −60mV for 400 milliseconds to deactivate M-type potassium channels. M-currents amplitudes were determined from this deactivation kinetics[12].

The sizes of MrgprX1 neurons were estimated by whole-cell capacitance (C_m):

$$C_m = C_M 4\pi r^2$$

Where typical membrane capacitance (C_M) is 0.01pF/μm^2.

Behavioral tests

Experiments were performed on sex-balanced, 8–12 week old mice (20 to 30 g) that had either been generated on a C57BL/6J background or backcrossed to C57BL/6J mice. On the day of the experiment, animals were first allowed to acclimatize to the test chamber for 10 min before injection. BAM8–22 (1mM) were subcutaneously injected into the nape of the neck (50 μL volume), and scratching behavior was observed for 30 min. A bout of scratching was defined as a continuous scratching movement with either hindpaw directed at the area of the injection site.

Statistics

Results are reported as mean ± S.E.M. Two-tailed t-tests, paired-sample t tests, Turkey HSD, or ANOVA were used to determine significance in statistical comparisons, and differences were considered significant at $p<0.05$. Statistical power analysis was used to justify sample size, and variance was determined to be similar among all treatment groups as determined by F test. No samples or animals subjected to successful procedures and/or treatments were excluded from analysis.

Author Manuscript Author Manuscript Author Manuscript Author Manuscript

Results

Activation of MrgprX1 triggers robust action potentials in PTX and PLC-dependent pathways.

To study the physiology of human MrgprX1 in native dorsal root ganglion (DRG) neurons, we used a recently generated humanized MrgprX1 mouse model in which twelve endogenous Mrgprs were replaced by human MrgprX1[9]. The expression of MrgprX1 was driven by MrgprC11 promoter. Since MrgprA3 expressing neurons are a subset of MrgprC11 expressing neurons, we used Cre-GFP driven by MrgprA3 promoter to label these MrgprX1 DRG neurons (Figure 1A). The MrgprX1 cells are small-diameter DRG neurons with an average diameter of 14.7 ± 0.11 μm (n=148) (Figure 1B). The averaged whole-cell capacitance is 27.2 ± 0.42 pF (n=148) and the averaged resting membrane potential is 61.9 ± 0.66 mV (n=75). It is known that several pruritogens including histamine and chloroquine can trigger action potential discharges in peripheral sensory neurons[5,6,13,14]. We found that application of BAM8–22 evoked robust action potential discharges in MrgprX1 DRG neurons without current injections. The concentration threshold for evoking action potentials was between 10 to 100 nanomolar (Figure 1C), a concentration that is comparable with previous calcium mobility studies[8,15-17]. We therefore used 100nM BAM8–22, which evoked 84±4.5 action potentials, as a default condition in the following experiments (Figure 1D). This BAM8–22 evoked firing was dependent on MrgprX1 as DRG neurons from Mrgpr knockout mice (MrgprA3 $^{GFP\text{-}cre}$ x Mrgprs $^{-/-}$) had no response to BAM8–22 (Figure 1E) or chloroquine (as shown in previous study[6]). To further identify downstream G-protein subunits, we used pertussis toxin (PTX, a $G\alpha_{i/o}$ subunit inhibitor), cholera toxin (CTX, a $G\alpha_{s}$ subunit inhibitor), and U73122 (a phospholipase C inhibitor) to dissect the downstream signal pathway. Pretreatment with CTX (2μg/mL) did not reduce BAM8–22 evoked action potentials (Figure 1F), however pretreatment with PTX (2μg/mL)[18] completely abolished BAM8–22 evoked action potential discharges (Figure 1G). Pretreatment with U73122 (10μM)[19] significantly reduced, although did not completely block, BAM8–22 evoked action potentials (Figure 1H&J). Application of 100uM Gallein[5], a $G\beta\gamma$ subunits blocker, almost completely inhibited action potential discharges (Figure 1I). The BAM8–22 evoked action potentials under different conditions were summarized in Figure 1J. Taken together, these results suggest MrgprX1 is coupled to PTX-sensitive and PLC pathways in a $G\beta\gamma$ dependent manner.

BAM8–22-elicited excitability is not caused by TRP, chloride or M-type K+ channels.

We next sought to identify the downstream ion channels responsible for triggering BAM8–22 induced neuronal firing. It is thought that MrgprA3 and MrgprC11 evoke neuronal activity by opening *Transient receptor potential* ankyrin 1 (Trpa1) channels, while histamine receptors activate neurons by opening *Transient receptor potential* vanilloid 1 (Trpv1) channels[5]. To our surprise, application of either 100μM HC030031[5], a selective TRPA1 blocker, or 10μM Ruthenium Red[6], a broad TRP channel blocker, had no inhibitory effects on BAM8–22 evoked action potentials. (Figure 2A-B). We suspected HC030031 might exhibit off-target blockage on VGCC, inhibiting calcium mobility. Indeed, both ruthenium red (10μM) and HC030031 (100μM) significantly inhibited voltage-gated calcium currents by 51 ± 0.04% and 32 ± 0.04%, respectively (Figure 2C-D). Other ion channels such as

Author Manuscript Author Manuscript Author Manuscript Author Manuscript

calcium activated chloride channels (CaCCs) and M-type potassium channels (KCNQ) have been reported as downstream effectors of GPCR-mediated neuronal excitability[13,20,21]. We tested the role of chloride channels by applying 4,4'-Diisothiocyano-2,2'-stilbenedisulfonic acid (*DIDS*), a commonly-used blocker for CaCCs and other chloride channels. Application of 100μM DIDS[22] did not significantly inhibit BAM8–22 evoked action potential discharges (Figure 2E). These blockers neither inhibited BAM8–22 evoked action potentials (Figure 2F) nor reduced the firing rates (Figure 2G). The peak firing rates under control (n=16), HC030031 (n=6), Ruthenium red (n=8), or DIDS (n=8) were 3.8 ± 0.41, 3.8 ± 0.37, 4.3 ± 0.75, or 3.0 ± 0.8 Hz, respectively. Application of 100nM BAM8–22 did not affect M-type potassium currents (Fig. 2H-I). Collectively, these results suggest that TRP, chloride or M-type potassium channels are not the downstream ion channel effectors of MrgprX1 activation.

BAM8–22 activates MrgprX1 DRG neurons by increasing the activity of TTX-resistant voltage-gated sodium channels.

Since TRP, KCNQ, and chloride channels are unlikely the downstream effectors for MrgprX1 mediated excitability, we re-examined the effects of BAM8–22 on membrane potentials. We found that, unlike chloroquine which depolarizes membrane potentials by about 9 mV[13], BAM8–22 evoked action potentials and inward sodium currents without depolarizing cell membranes (Figure 3A-C). We suspected that MrgprX1 can directly activate voltage-gated sodium channel, but to our surprise, application of 500nM tetrodotoxin (TTX) could not completely block BAM8–22 evoked action potentials (Figure 3D). However, the number of action potentials in the presence of TTX was significantly reduced (Figure 3F). Furthermore, lidocaine (500μM) completely blocked action potential discharges (Figure 3E). These results suggest BAM8–22 evoked action potentials are contributed by TTX-resistant sodium channels, Nav1.8 and Nav1.9. To further investigate the biophysical properties of TTX-resistant sodium channels in response to MrgprX1 activation, we used a voltage protocol to isolate TTX-resistant sodium currents[11]. We found that BAM8–22 augmented and acutely activated persistent sodium currents (Figure 3G), leading to a hyperpolarized shift on steady-state activation curves by about 5–7mV (Figure 3H). In the presence of 100nM or 10μM BAM8–22, the half-maximum activation voltage ($V_{1/2}$) shifted from −23.5 ± 0.28mV to −28.9 ± 0.32mV, or −31.2 ± 0.97mV, respectively (Figure 3H). Application of BAM8–22 did not notably increase the current density of TTX-resistant sodium channels (Figure 3I). The hyperpolarized shifting on voltage dependency of TTX-resistant sodium channels requires MrgprX1 as in the knockout DRG neurons ($MrgprA3^{GFP\text{-}cre}$ x Mrgpr $^{-/-}$), BAM8–22 did not significantly shift the activation curves of TTX-resistant sodium channels. The $V_{1/2}$ values of activation curves in the absence and presence of 100nM and 10μM BAM8–22 were −28.4 ± 1.0mV, −29.9 ± 1.0mV, −30.8 ± 1.2mV, respectively (Figure 3J). To further test the role of Trpa1 and TTX-resistant sodium channels in BAM8–22 evoked itch, we performed behavioral tests on Na1.9 knockout (gifts from Dr. Frank Bosmans)[23] or Trpa1 knockout mice (The Jackson Laboratory). Compared to wildtype mice in which BAM8–22 evoked 28.1 ± 4.1 scratching bouts within 30 minutes, the Nav1.9 knockout mice showed a significant reduction in scratching bouts (9.1 ± 3.6). Moreover, BAM8–22 evoked scratching bouts were not decreased in Trpa1 knockout mice (27.9 ± 6.3) (Figure 3K). Collectively, these data suggest that BAM8–22 evoked neuronal

Author Manuscript Author Manuscript Author Manuscript Author Manuscript

excitability and itch is likely through direct modulation on the activity of TTX-resistant sodium channels.

Discussion

Activation of certain Mrgprs including MrgprA3, MrgprC11, and MrgprD elicits itch sensation by increasing neuronal excitability of DRG neurons[5,6,10,13,24]. It is thought that activation of MrgprA3 or MrgprC11 opens TRPA1 and triggers neuronal firing resulting in itch[5]. However, a recent study shows that MrgprA3 mediated neuronal firing and itch behavior do not require TRPA1 or TRPV1 channels[13]. Paradoxically, several groups independently showed TRPA1 blocker HC030031 effectively inhibited chloroquine (a MrgprA3 agonist) induced calcium mobility in DRG neurons[5,25,26]. How can a TRPA1 blocker antagonize neuronal activity when TRPA1 is not involved in that process? It has been shown that ruthenium red can block not only TRP channels but also other ion channels including ryanodine receptors[27], mechanosensitive channels Piezo2[28] and voltage-gated calcium channels (VGCC)[29] with IC_{50} values ranging from high nanomolar to low micromolar. We suspected HC030031 may inhibit VGCC as well, indeed we found both blockers effectively inhibited VGCC currents. This result suggests that these TRP channel blockers could interfere with the interpretation of calcium imaging experiments. In general, our electrophysiological and behavioral studies support the conclusion that TRP channels are not the downstream effectors for MrgprX1, MrgprC11, or MrgprA3. However, whether TRP channels couples to other Mrgprs such as MrgprX2, MrgprB2, or MrgprD requires further investigation. Our electrophysiological study revealed that MrgprX1 activation can induce inward sodium currents and can reduce the activation threshold of TTX-resistant sodium channels. TTX-resistant sodium channels, Nav1.8 and Nav1.9, are considered peripheral sodium channels as their expression is restricted to peripheral sensory neurons[30]. Ample evidence has shown that TTX-resistant sodium channels contribute to neuronal hyperexcitability during chronic and inflammatory pain. For example, several G-protein coupled receptor agonists including Bradykinin, prostaglandin E2 (PGE2), serotonin, adenosine, and CCL-2 as well as cytokine including TNF-α and interleukin-1, increase TTX-resistant sodium channel activity resulting in pain hyper-sensitivity[11,31-34,35(p9),36]. Furthermore, other studies show that this GPCR modulation is through a PTX-sensitive and Gβγ dependent pathway[11,31]. It has also been reported that Gβγ subunits can directly bind to the C-terminus of sodium channels and induce persistent sodium currents[37,38]. In our study, although BAM8–22 only reduces the activation threshold of TTX-resistant sodium channels by 5–7mV, it is worth noting that a Nav1.8 point mutation, A1304T, identified from patients with painful neuropathy has a similar degree (6mV) of hyperpolarized shift in activation $V_{1/2}$ value[39]. We noted that in Mrgpr-cluster knockout mice, the activation threshold of TTX-resistant sodium channels is about 5mV lower than that of the MrgprX1 mice. There might be a potential coupling between MrgprX1 and voltage-gated sodium channels which tunes basal neuronal excitability. The importance of TTX-resistant sodium channels in itch can be highlighted by a mutation in SCN11A (Nav1.9). Patients with the mutation (L811P) suffer severe itch[42(p9)]. Mice carrying the same mutation also show increased spontaneous scratching behavior[23]. Moreover, single-cell RT-PCR showed chloroquine-responsive neurons, presumably MrgprA3 neurons, preferentially express

Author Manuscript Author Manuscript Author Manuscript Author Manuscript

Nav1.9 and Nav1.8 over other Nav subunits[41]. Single cell RNA-Seq data also showed both Nav1.8 and Nav1.9 are preferentially enriched in itch-related DRG neurons including MrgprA3, Nppb, and MrgprD neurons[42]. Based on these lines of evidence, we concluded that TTX-resistant sodium channels are the downstream effectors for MrgprX1 and perhaps MrgprC11.

Acknowledgment

We thank Dr. Liang Han, Dr. Yixun Geng for generating and maintaining transgenic mouse lines. This work was supported by NIH and HHMI grants to XD. PYT current affiliation is National Institute of Dental and Craniofacial Research at National Institute of Health.

Reference

1. Solinski HJ, Gudermann T, Breit A. Pharmacology and signaling of MAS-related G protein-coupled receptors. Pharmacol Rev. 2014;66(3):570–597. doi:10.1124/pr.113.008425 [PubMed: 24867890]
2. Liu Q, Dong X. The role of the Mrgpr receptor family in itch Handb Exp Pharmacol. 2015;226:71–88. doi:10.1007/978-3-662-44605-8_5 [PubMed: 25861775]
3. Meixiong J, Dong X. Mas-Related G Protein–Coupled Receptors and the Biology of Itch Sensation. Annu Rev Genet. 2017;51(1):103–121. doi:10.1146/annurev-genet-120116-024723 [PubMed: 29178819]
4. Sikand P, Dong X, LaMotte RH. BAM8–22 peptide produces itch and nociceptive sensations in humans independent of histamine release. J Neurosci. 2011;31(20):7563–7567. doi:10.1523/JNEUROSCI.1192-11.2011 [PubMed: 21593341]
5. Wilson SR, Gerhold KA, Bifolck-Fisher A, et al. TRPA1 is required for histamine-independent, Mas-related G protein-coupled receptor-mediated itch. Nat Neurosci. 2011;14(5):595–602. doi:10.1038/nn.2789 [PubMed: 21460831]
6. Liu Q, Tang Z, Surdenikova L, et al. Sensory neuron-specific GPCR Mrgprs are itch receptors mediating chloroquine-induced pruritus. Cell. 2009;139(7):1353–1365. doi:10.1016/j.cell.2009.11.034 [PubMed: 20004959]
7. Solinski HJ, Petermann F, Rothe K, Boekhoff I, Gudermann T, Breit A. Human Mas-related G protein-coupled receptors-X1 induce chemokine receptor 2 expression in rat dorsal root ganglia neurons and release of chemokine ligand 2 from the human LAD-2 mast cell line. PloS One. 2013;8(3):e58756. doi:10.1371/journal.pone.0058756 [PubMed: 23505557]
8. Wen W, Wang Y, Li Z, et al. Discovery and Characterization of 2-(Cyclopropanesulfonamido)-N-(2-ethoxyphenyl)benzamide, ML382: a Potent and Selective Positive Allosteric Modulator of MrgX1. ChemMedChem 2015;10(1):57–61. doi:10.1002/cmdc.201402277 [PubMed: 25209672]
9. Li Z, Tseng P-Y, Tiwari V, et al. Targeting human Mas-related G protein-coupled receptor X1 to inhibit persistent pain. Proc Natl Acad Sci U S A. 2017;114(10):E1996–E2005. doi:10.1073/pnas.1615255114 [PubMed: 28223516]
10. Han L, Ma C, Liu Q, et al. A subpopulation of nociceptors specifically linked to itch. Nat Neurosci. 2013;16(2):174–182. doi:10.1038/nn.3289 [PubMed: 23263443]
11. Belkouch M, Dansereau MA, Reaux-Le Goazigo A, et al. The chemokine CCL2 increases Nav1.8 sodium channel activity in primary sensory neurons through a Gbetagamma-dependent mechanism. J Neurosci. 2011;31(50):18381–18390. doi:10.1523/JNEUROSCI.3386-11.2011 [PubMed: 22171040]
12. Chen H, Ikeda SR. Modulation of ion channels and synaptic transmission by a human sensory neuron-specific G-protein-coupled receptor, SNSR4/mrgX1, heterologously expressed in cultured rat neurons. J Neurosci. 2004;24(21):5044–5053. doi:10.1523/JNEUROSCI.0990-04.2004 [PubMed: 15163697]
13. Ru F, Sun H, Jurcakova D, et al. Mechanisms of pruritogen-induced activation of itch nerves in isolated mouse skin. J Physiol. 2 2017. doi:10.1113/JP273795

Author Manuscript Author Manuscript Author Manuscript Author Manuscript

14. Taylor-Clark TE, Nassenstein C, Undem BJ. Leukotriene D4 increases the excitability of capsaicin-sensitive nasal sensory nerves to electrical and chemical stimuli. Br J Pharmacol. 2008;154(6):1359–1368. doi:10.1038/bjp.2008.196 [PubMed: 18500362]
15. Lembo PM, Grazzini E, Groblewski T, et al. Proenkephalin A gene products activate a new family of sensory neuron--specific GPCRs. Nat Neurosci. 2002;5(3):201–209. doi:10.1038/nn815 [PubMed: 11850634]
16. Burstein ES, Ott TR, Feddock M, et al. Characterization of the Mas-related gene family: structural and functional conservation of human and rhesus MrgX receptors. Br J Pharmacol. 2006;147(1):73–82. doi:10.1038/sj.bjp.0706448 [PubMed: 16284629]
17. Kunapuli P, Lee S, Zheng W, et al. Identification of small molecule antagonists of the human mas-related gene-X1 receptor. Anal Biochem. 2006;351(1):50–61. doi:10.1016/j.ab.2006.01.014 [PubMed: 16510108]
18. Bourinet E, Soong TW, Stea A, Snutch TP. Determinants of the G protein-dependent opioid modulation of neuronal calcium channels. Proc Natl Acad Sci U S A. 1996;93(4):1486–1491. doi:10.1073/pnas.93.4.1486 [PubMed: 8643659]
19. Macmillan D, McCarron JG. The phospholipase C inhibitor U-73122 inhibits Ca(2+) release from the intracellular sarcoplasmic reticulum Ca(2+) store by inhibiting Ca(2+) pumps in smooth muscle. Br J Pharmacol. 2010;160(6):1295–1301. doi:10.1111/j.1476-5381.2010.00771.x [PubMed: 20590621]
20. Liu B, Linley JE, Du X, et al. The acute nociceptive signals induced by bradykinin in rat sensory neurons are mediated by inhibition of M-type K+ channels and activation of Ca2+-activated Cl– channels. J Clin Invest. 2010;120(4):1240–1252. doi:10.1172/JCI41084 [PubMed: 20335661]
21. Crozier RA, Ajit SK, Kaftan EJ, Pausch MH. MrgD Activation Inhibits KCNQ/M-Currents and Contributes to Enhanced Neuronal Excitability. J Neurosci. 2007;27(16):4492. doi:10.1523/JNEUROSCI.4932-06.2007 [PubMed: 17442834]
22. Schroeder BC, Cheng T, Jan YN, Jan LY. Expression Cloning of TMEM16A as a Calcium-Activated Chloride Channel Subunit. Cell. 2008;134(6):1019–1029. doi:10.1016/j.cell.2008.09.003 [PubMed: 18805094]
23. Salvatierra J, Diaz-Bustamante M, Meixiong J, Tierney E, Dong X, Bosmans F. A disease mutation reveals a role for NaV1.9 in acute itch. J Clin Invest. 2018;128(12):5434–5447. doi:10.1172/JCI122481 [PubMed: 30395542]
24. Liu Q, Sikand P, Ma C, et al. Mechanisms of itch evoked by beta-alanine. J Neurosci. 2012;32(42):14532–14537. doi:10.1523/JNEUROSCI.3509-12.2012 [PubMed: 23077038]
25. Roberson DP, Gudes S, Sprague JM, et al. Activity-dependent silencing reveals functionally distinct itch-generating sensory neurons. Nat Neurosci. 2013;16(7):910–918. [PubMed: 23685721]
26. Than JY, Li L, Hasan R, Zhang X. Excitation and modulation of TRPA1, TRPV1, and TRPM8 channel-expressing sensory neurons by the pruritogen chloroquine. J Biol Chem. 2013;288(18):12818–12827. doi:10.1074/jbc.M113.450072 [PubMed: 23508958]
27. Ma J Block by ruthenium red of the ryanodine-activated calcium release channel of skeletal muscle. J Gen Physiol. 1993;102(6):1031–1056. [PubMed: 7510773]
28. Coste B, Xiao B, Santos JS, et al. Piezo proteins are pore-forming subunits of mechanically activated channels. Nature. 2012;483(7388):176–181. doi:10.1038/nature10812 [PubMed: 22343900]
29. Cibulsky SM, Sather WA. Block by ruthenium red of cloned neuronal voltage-gated calcium channels. J Pharmacol Exp Ther. 1999;289(3):1447–1453. [PubMed: 10336538]
30. Waxman SG, Zamponi GW. Regulating excitability of peripheral afferents: emerging ion channel targets. Nat Neurosci. 2014;17(2):153–163. doi:10.1038/nn.3602 [PubMed: 24473263]
31. Rush AM, Waxman SG. PGE2 increases the tetrodotoxin-resistant Nav1.9 sodium current in mouse DRG neurons via G-proteins. Brain Res. 2004;1023(2):264–271. doi:10.1016/j.brainres.2004.07.042 [PubMed: 15374752]
32. Binshtok AM, Wang H, Zimmermann K, et al. Nociceptors Are Interleukin-1β Sensors. J Neurosci. 2008;28(52):14062. doi:10.1523/JNEUROSCI.3795-08.2008 [PubMed: 19109489]

Author Manuscript Author Manuscript Author Manuscript Author Manuscript

33. Gold MS, Reichling DB, Shuster MJ, Levine JD. Hyperalgesic agents increase a tetrodotoxin-resistant Na+ current in nociceptors. Proc Natl Acad Sci U S A. 1996;93(3):1108–1112. [PubMed: 8577723]
34. Gudes S, Barkai O, Caspi Y, Katz B, Lev S, Binshtok AM. The role of slow and persistent TTX-resistant sodium currents in acute tumor necrosis factor-α-mediated increase in nociceptors excitability. J Neurophysiol. 2015;113(2):601. doi:10.1152/jn.00652.2014 [PubMed: 25355965]
35. Amaya F, Wang H, Costigan M, et al. The voltage-gated sodium channel Na(v)1.9 is an effector of peripheral inflammatory pain hypersensitivity. J Neurosci. 2006;26(50):12852–12860. doi:10.1523/JNEUROSCI.4015-06.2006 [PubMed: 17167076]
36. Gold MS, Levine JD, Correa AM. Modulation of TTX-R I Na by PKC and PKA and Their Role in PGE2-Induced Sensitization of Rat Sensory Neurons In Vitro. J Neurosci. 1998;18(24):10345. [PubMed: 9852572]
37. Ma JY, Catterall WA, Scheuer T. Persistent sodium currents through brain sodium channels induced by G protein betagamma subunits. Neuron. 1997;19(2):443–452. [PubMed: 9292732]
38. Mantegazza M, Yu FH, Powell AJ, Clare JJ, Catterall WA, Scheuer T. Molecular Determinants for Modulation of Persistent Sodium Current by G-Protein βγ Subunits. J Neurosci. 2005;25(13):3341. doi:10.1523/JNEUROSCI.0104-05.2005 [PubMed: 15800189]
39. Faber CG, Lauria G, Merkies ISJ, et al. Gain-of-function Na(v)1.8 mutations in painful neuropathy. Proc Natl Acad Sci U S A. 2012;109(47):19444–19449. doi:10.1073/pnas.1216080109 [PubMed: 23115331]
40. Woods CG, Babiker MOE, Horrocks I, Tolmie J, Kurth I. The phenotype of congenital insensitivity to pain due to the NaV1.9 variant p.L811P. Eur J Hum Genet. 2015;23:1434.
41. Jurcakova D, Ru F, Kollarik M, Sun H, Krajewski J, Undem BJ. Voltage-Gated Sodium Channels Regulating Action Potential Generation in Itch-, Nociceptive-, and Low-Threshold Mechanosensitive Cutaneous C-Fibers. Mol Pharmacol. 2018;94(3):1047. doi:10.1124/mol.118.112839 [PubMed: 29941667]
42. Usoskin D, Furlan A, Islam S, et al. Unbiased classification of sensory neuron types by large-scale single-cell RNA sequencing. Nat Neurosci. 2015;18(1):145–153. doi:10.1038/nn.3881 [PubMed: 25420068]

Author Manuscript Author Manuscript Author Manuscript Author Manuscript

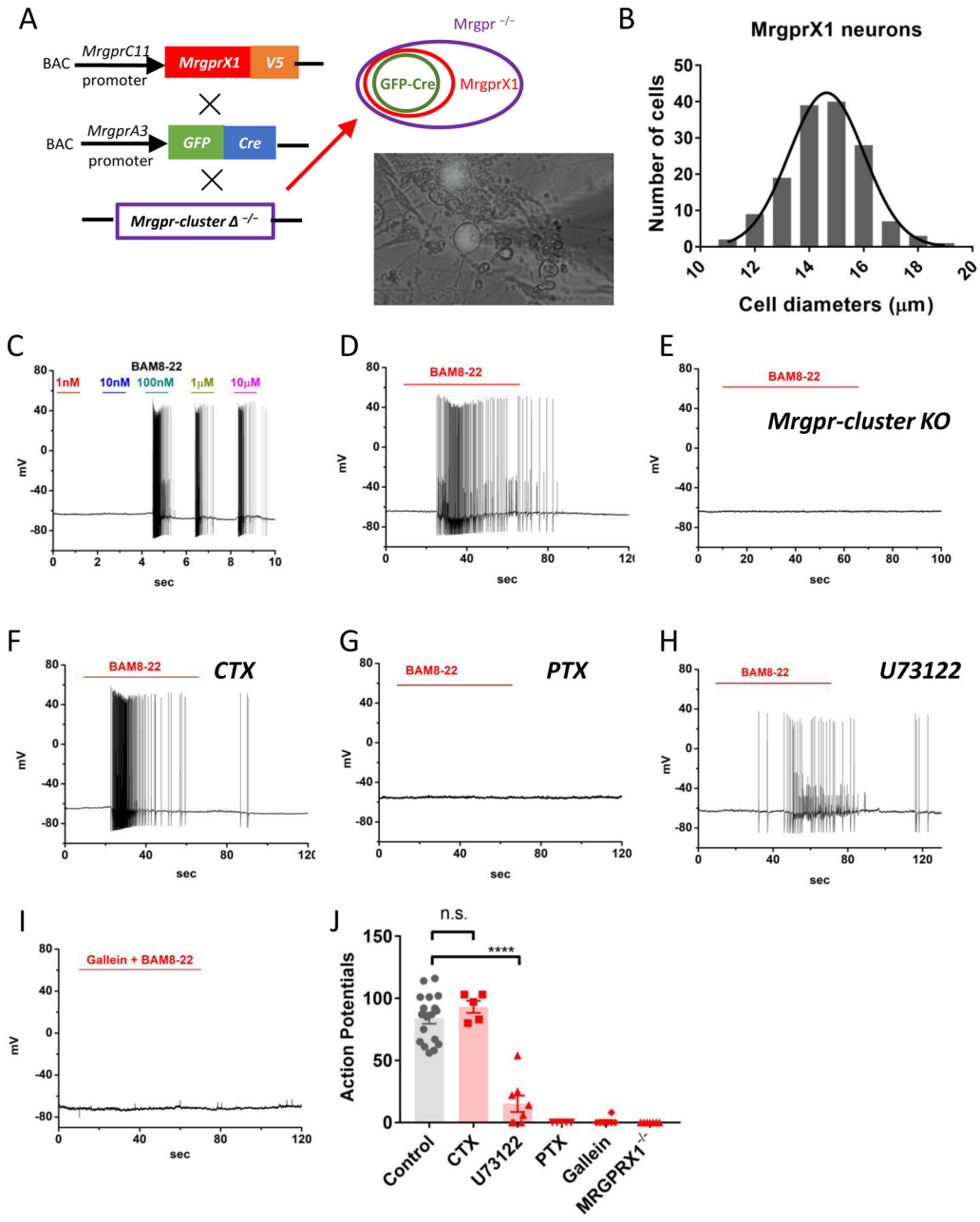

Figure 1. Activation of MrgprX1 triggers robust action potential discharges in dorsal root ganglion neurons.

(A) Strategy for generating the BAC transgenic line expressing human MrgprX1 driven by mouse MrgprC11promoter. The Mrgprc11 MrgprX1 transgenic mice were mated with Mrgpra3GFP-Cretransgenic mice and then crossed into the Mrgpr-cluster Δ−/−background. Since Mrgpra3 is a subpopulation of Mrgprc11, the GFP-cre will label a subset of MrgprX1 neurons. The purple circle indicates all DRG neurons that lacked the 12 endogenous mouse Mrgprs. The red circle indicates a subpopulation of all MrgprX1 neurons. The green circle indicates the neurons that expressed both MrgprX1 and Cre-GFP. The lower-right picture shows the MrgprX1 DRG neurons that expressed Cre-GFP in the nuclei. (B) The estimated

Author Manuscript Author Manuscript Author Manuscript Author Manuscript

sizes of MrgprX1 cells. The average diameter is 14.7 ± 0.11 μm (n=148). (C) A sample current-clamp recording of MrgprX1 neurons at different concentrations of BAM8-22 (n=3). (D) A sample recording of MrgprX1 neurons in the presence of 100nM for one minute (n=18). (E) A sample recording from Cre-GFP labeled, Mrgpr-cluster Δ −/−(MrgprX1−/−) DRG neurons in the presence of 100nM BAM8-22 (n=7). (F) Pretreatment with cholera toxin (2μg/mL) overnight had no effects on BAM8-22 evoked action potentials (n=5). (G) Pertussis toxin pretreatment (2μg/mL, overnight) completely block BAM8-22 evoked excitability (n=5). (H) Pretreatment with U73122 for 5 minutes greatly reduced, but did not prevent, BAM8-22 mediated excitability (n=8). (I) A Gβγ subunit inhibitor, Gallein (100μM), completely blocked BAM8-22 induced action potential discharges (n=8). (J) Summarized data for total action potentials discharges induced by 100nM BAM8-22 under different conditions. Data were presented as mean ± s.e.m., **** p=0.0001, by two-tailed t test.

Author Manuscript Author Manuscript Author Manuscript Author Manuscript

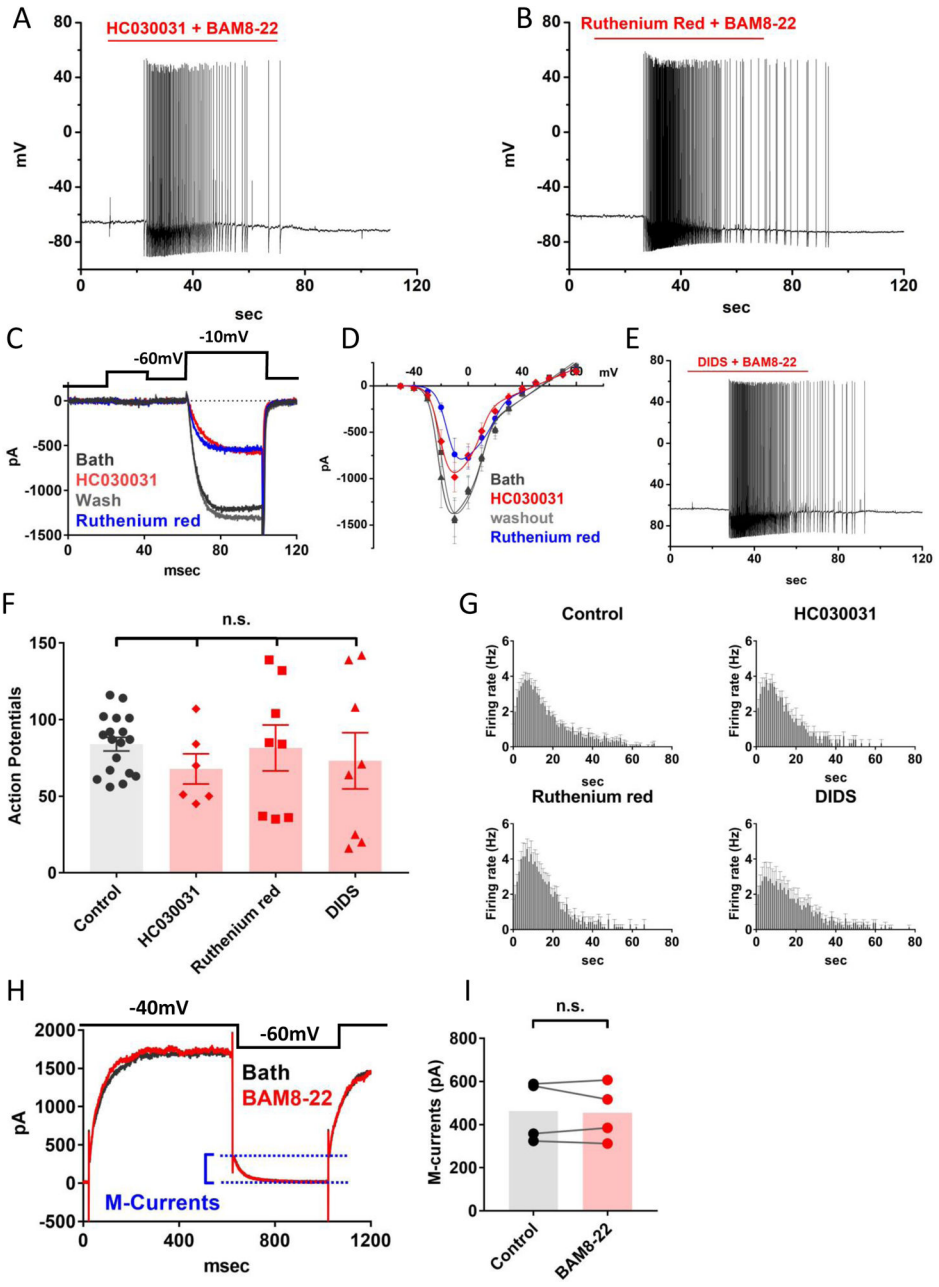

Figure 2. MrgprX1-mediated neuronal firing does not require TRPA1 or other TRP channels.

(A) A sample recording of BAM8-22 evoked action potentials in the presence of 100μM HC030031. (B) BAM8-22 elicited action potentials in the presence of 10μM ruthenium red. (C) Ruthenium red (10μM) and HC030031 (100μM) significantly inhibited voltage-gated calcium currents. (D) The current inhibition at −10mV in the presence of ruthenium red or HC030031 was 51±0.04% (n=5, p=0.002), or 32±0.04% (n=5, p=0.01), respectively. Statistics were performed with paired-sample t-test. The current inhibitions were plotted as the function of membrane potentials and were fitted with Boltzmann IV equation. (E) A sample recording showing that DIDS (10μM), a broad-spectrum chloride channel blocker, does not block BAM8-22 elicited action potentials. (F) Summary of the number of

Author Manuscript Author Manuscript Author Manuscript Author Manuscript

BAM8-22 evoked action potentials in the presence of differing ion channel blockers and control condition. HC030031 (n=6, p=0.11), Ruthenium red (n=8, p=0.84), DIDS (n=8, p=0.44). Statistics were performed with a two-tailed t-test. (G) Plots of BAM8-22 evoked firing rates as the function of time. The treatments of HC030031, Ruthenium red, or DIDS did not significantly reduce the peak firing rate, p values are 0.99, 0.56, or 0.33, respectively. statistics were performed with two-tailed t-test. (H) Sample traces of M-type potassium currents recordings. M-current amplitudes were estimated between two dashed lines. (I) BAM8-22 (100nM) had no noticeable effects on M-currents (p=0.73, paired-sample t-test).

Author Manuscript Author Manuscript Author Manuscript Author Manuscript

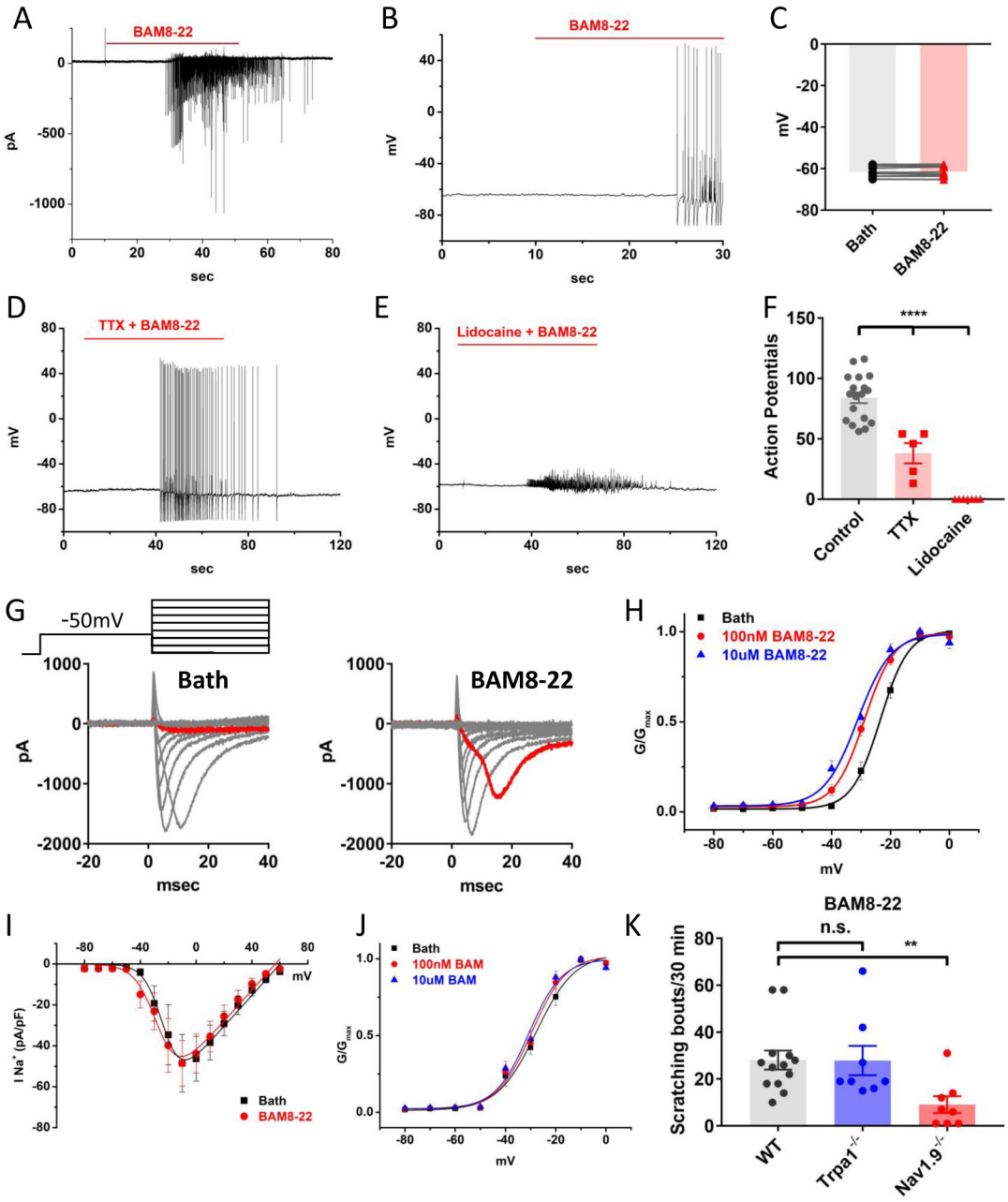

Figure 3. Activation of MrgprX1 increased the activity of TTX-resistant voltage-gated sodium channels.

(A) Sample recording of BAM8-22 induced fast-transient inward currents under voltage clamp (holding at −60mV, n=8). (B) Sample current-clamp recordings show BAM8-22 evokes action potentials without depolarizing cell membranes. (C) The membrane potentials in the presence of 100nM BAM8-22 (−61.53mV) and before BAM8-22 (−61.61mV) were not significantly different (p=0.5, n=8, paired-sampled t-test) (D) BAM8-22 elicited neuronal firing was not blocked by the sodium channel blocker TTX (500nM). (E) Lidocaine (500 μM) completely inhibited BAM8-22 evoked action potentials (n=7). (F) Summary of the effects of TTX and lidocaine on BAM8-22 evoked action potentials.

Author Manuscript Author Manuscript Author Manuscript Author Manuscript

Although TTX did not completely block BAM8-22 evoked firing, it significantly reduced the number of evoked action potentials (n=5, p=0.0001, two-tailed t-test). (G) Sample recordings of TTX-resistant sodium currents in the absence (left) and the presence (right) of 100nM BAM8-22. BAM8-22 treatment augmented TTX-R sodium currents at −20mV (highlighted by red). (H) Steady-state voltage dependency of TTX-R sodium channels. BAM8-22 treatment significantly shifted the half maximum activation voltages ($V_{1/2}$)to more hyperpolarized direction. The $V_{1/2}$ values of control, 100nM and 10μM BAM8-22 were −23.5±0.28mV, −28.9±0.32mV, −31.2±0.97mV, respectively (n=11, P=0.001, Turkey HSD). (I) The TTX-R sodium current densities (currents normalized with whole-cell capacitance, pA/pF) plotted as the function of voltage. Peak current densities under control (35.2±5.4) and 100nM BAM8-22 (37.8±5.1) were not significantly different (n=5, p=0.3, paired-sampled t-test). (J) In the absence of MrgprX1 (from GFP-cre+, *Mrgpr-cluster Δ −/−* mice), BAM8-22 did not change steady-state voltage dependency of TTX-R sodium channels. The $V_{1/2}$ values in control, 100nM and 10μM BAM8-22 were −28.4 ±1.0mV, −29.9±1.0mV, −30.8±1.2mV, respectively (n=7, p=0.3, Turkey HSD). (K) BAM8-22 (1mM, 50μL in napes) evoked scratching bouts were reduced in Nav1.9 knockout but not Trpa1 knockout mice (wildtype n=13; Nav1.9 KO n=8, p=0.005; Trpa1 KO n=8, p=0.98; two-tailed-t-test).